Cancer Cell

CellPress

Letter

Mutations in IFN-γ signaling genes sensitize tumors to immune checkpoint blockade

Eric Song[1,2] and Ryan D. Chow[3,4,*]
[1]Department of Immunobiology, Yale University School of Medicine, New Haven, CT, USA
[2]Department of Ophthalmology, Yale University School of Medicine, New Haven, CT, USA
[3]Department of Genetics, Yale University School of Medicine, New Haven, CT, USA
[4]Lead contact
*Correspondence: ryan.chow@yale.edu
https://doi.org/10.1016/j.ccell.2023.02.013

Most tumors are resistant to immune checkpoint blockade (ICB). Interferon gamma (IFN-γ) is an anti-tumor cytokine produced by immune cells, and prior clinical reports have identified IFN-γ signaling pathway alterations in tumors with primary[1,2] or acquired[3] resistance to ICB. However, these studies lacked the statistical power to ascertain whether alterations in IFN-γ signaling genes are significantly associated with ICB resistance. In light of our recent observation that endometrial carcinomas with pre-treatment loss-of-function mutations in the IFN-γ signaling factor *JAK1* could still have robust responses to ICB,[4] we wondered whether the relationship between IFN-γ signaling gene alterations and anti-tumor immunity may be more complex than commonly appreciated.

We first compiled functional genomic data investigating the impact of IFN-γ signaling gene alterations on anti-tumor immunity, assembling a total of 33 CRISPR screens (Table S1). 19 of these screens utilized *in vitro* co-culture models, in which target tumor cells were incubated together with effector immune cells. The remaining 14 screens were based on *in vivo* tumor transplantation models in mice, comparing immunodeficient and immunocompetent hosts. We examined whether tumor-intrinsic mutations in *JAK1*, *JAK2*, *IFNGR1*, *IFNGR2*, and *STAT1* (constituting the core IFN-γ signaling pathway) were under positive or negative selection in the presence of anti-tumor immune pressure.

Among *in vitro* co-culture models, 17 of 19 (89.5%) screens showed enrichment for multiple IFN-γ signaling gene alterations, indicating enhanced resistance to anti-tumor immunity upon loss of IFN-γ signaling (Figure S1A). Specifically, ≥2 IFN-γ signaling gene alterations were enriched in 13 of 13 (100%) T cell co-culture screens, 1 of 2 (50%) CAR-T screens, and 3 of 4 (75%) natural killer cell screens. In contrast to the *in vitro* screens, only 3 of 14 (21.4%) *in vivo* tumor screens demonstrated positive selection for alterations in IFN-γ signaling genes in the setting of host immune pressure (Figure S1B). Alterations in IFN-γ signaling genes were significantly less likely to be enriched *in vivo* compared to *in vitro* ($p = 0.0002$). Conversely, 9 of 14 (64.3%) *in vivo* screens showed significant depletion of IFN-γ signaling gene alterations in the presence of immune pressure, compared to 1 of 19 (5.3%) *in vitro* screens ($p = 0.0004$). Our meta-analysis of 33 CRISPR screens thus demonstrated that IFN-γ signaling gene alterations have opposing effects on anti-tumor immunity *in vitro* vs. *in vivo*.

Given that prior studies have implicated mutations in IFN-γ signaling genes as drivers of ICB resistance in patients,[1–3] it was unclear how to reconcile these reports with our analysis of multiple *in vivo* CRISPR screens pointing to the contrary. As all of the *in vivo* CRISPR screens included in our analysis were conducted in mice, we sought to investigate the impact of alterations in IFN-γ signaling genes in a clinical setting. Drawing from 29 studies, we constructed a clinicogenomic cohort of ICB-treated patients whose tumors were sequenced prior to initiating treatment. Our complete cohort consisted of 2,154 ICB-treated patients encompassing cancers from 7 different tissues (Table S1).

We conducted a mixed-effects meta-analysis evaluating the relationship between pre-treatment IFN-γ signaling gene alterations and ICB response, accounting for tumor mutation burden (TMB) at the patient level and cancer type at the cohort level. In the mixed-effects model (Cochran's $Q = 18.71$, heterogeneity test $p = 0.60$, overall $I^2 = 0$), alterations in IFN-γ signaling genes were significantly associated with higher odds of ICB response (adjusted log OR = 0.46, 95% confidence interval [CI] [0.09–0.83], $p = 0.016$) (Figure S1C; Table S1). As a validation of the model, higher TMB was also associated with ICB responsiveness (adjusted log OR = 0.80 [0.55–1.06], $p = 6.3*10^{-10}$), consistent with prior reports. We further conducted a sensitivity analysis in which we excluded mutations that were computationally predicted to have minimal effects on protein function.[5,6] This analysis similarly showed that tumors with "predicted pathogenic" alterations in IFN-γ signaling genes were more likely to respond to ICB (ESM1b predictor: adjusted log OR = 0.48, 95% CI [0.06–0.90], $p = 0.024$; EVE predictor: adjusted log OR = 0.56 [0.17–0.96], $p = 0.005$) (Table S1).

Our findings provide clarity regarding the functional impact of IFN-γ signaling gene alterations on anti-tumor immunity. In multiple *in vitro* co-culture systems, loss of IFN-γ signaling in tumor cells conferred resistance against effector immune cells. However, across diverse *in vivo* murine tumor models, IFN-γ signaling gene alterations sensitized tumors to the host immune system, with the caveat that there was some variability across *in vivo* screens (particularly for melanoma). Our study thus builds on prior work[7] by illuminating an experimentally reproducible dichotomy in how IFN-γ signaling gene alterations influence anti-tumor immunity *in vitro* compared to *in vivo*. In light of these observations, we revisited whether mutations in IFN-γ signaling genes are indeed associated with primary ICB resistance in the clinical

setting. To that end, our meta-analysis of 2,154 ICB-treated patients indicated that pre-treatment IFN-γ signaling gene alterations do not necessarily preclude responses to ICB.[4] Instead, pre-treatment alterations in IFN-γ signaling genes were significantly associated with enhanced ICB responsiveness, independently of TMB. Moving forward, it will be of interest to evaluate whether these findings differ in the context of acquired ICB resistance.

A limitation of our study is that the clinical associations described here do not necessarily indicate causality. However, when considered in conjunction with the functional genomics analyses, the collective experimental and clinical evidence indicates that, rather than conferring primary resistance to ICB, pre-treatment mutations in IFN-γ signaling genes may in fact sensitize tumors to ICB.[8–10] As our conclusions differ from those of prior reports, we speculate that larger and more diverse clinicogenomic cohorts are essential to unravel the complex role of IFN-γ signaling in anti-tumor immunity. Our study therefore highlights the potential for functional genomic and clinicogenomic meta-analyses to advance our understanding of the interplay between genetic alterations and responses to cancer therapy.

SUPPLEMENTAL INFORMATION

Supplemental information can be found online at https://doi.org/10.1016/j.ccell.2023.02.013.

ACKNOWLEDGMENTS

R.D.C. is supported by the NIH/NCI (F30CA250249, T32GM136651) and the Paul & Daisy Soros Fellowship. E.S. is supported by Yale School of Medicine Dean's Support for this work. The authors thank Jiping Wang and Shuangge Ma for statistical support.

DECLARATION OF INTERESTS

The authors declare no competing interests.

REFERENCES

1. Shin, D.S., Zaretsky, J.M., Escuin-Ordinas, H., Garcia-Diaz, A., Hu-Lieskovan, S., Kalbasi, A., Grasso, C.S., Hugo, W., Sandoval, S., Torrejon, D.Y., et al. (2017). Primary Resistance to PD-1 Blockade Mediated by JAK1/2 Mutations. Cancer Discov. *7*, 188–201. https://doi.org/10.1158/2159-8290.CD-16-1223.

2. Gao, J., Shi, L.Z., Zhao, H., Chen, J., Xiong, L., He, Q., Chen, T., Roszik, J., Bernatchez, C., Woodman, S.E., et al. (2016). Loss of IFN-γ Pathway Genes in Tumor Cells as a Mechanism of Resistance to Anti-CTLA-4 Therapy. Cell *167*, 397–404.e9. https://doi.org/10.1016/j.cell.2016.08.069.

3. Zaretsky, J.M., Garcia-Diaz, A., Shin, D.S., Escuin-Ordinas, H., Hugo, W., Hu-Lieskovan, S., Torrejon, D.Y., Abril-Rodriguez, G., Sandoval, S., Barthly, L., et al. (2016). Mutations Associated with Acquired Resistance to PD-1 Blockade in Melanoma. N. Engl. J. Med. *375*, 819–829. https://doi.org/10.1056/NEJMoa1604958.

4. Chow, R.D., Michaels, T., Bellone, S., Hartwich, T.M.P., Bonazzoli, E., Iwasaki, A., Song, E., and Santin, A.D. (2022). Distinct mechanisms of mismatch repair deficiency delineate two modes of response to PD-1 immunotherapy in endometrial carcinoma. Cancer Discov. *13*, 312–331. CD-22-0686. https://doi.org/10.1158/2159-8290.

5. Frazer, J., Notin, P., Dias, M., Gomez, A., Min, J.K., Brock, K., Gal, Y., and Marks, D.S. (2021). Disease variant prediction with deep generative models of evolutionary data. Nature *599*, 91–95. https://doi.org/10.1038/s41586-021-04043-8.

6. Brandes, N., Goldman, G., Wang, C.H., Ye, C.J., and Ntranos, V. (2022). Genome-wide prediction of disease variants with a deep protein language model. Preprint at bioRxiv. https://doi.org/10.1101/2022.08.25.505311.

7. Vredevoogd, D.W., Apriamashvili, G., and Peeper, D.S. (2021). The (re)discovery of tumor-intrinsic determinants of immune sensitivity by functional genetic screens. Immunooncol. Technol. *11*, 100043. https://doi.org/10.1016/j.iotech.2021.100043.

8. Benci, J.L., Johnson, L.R., Choa, R., Xu, Y., Qiu, J., Zhou, Z., Xu, B., Ye, D., Nathanson, K.L., June, C.H., et al. (2019). Opposing Functions of Interferon Coordinate Adaptive and Innate Immune Responses to Cancer Immune Checkpoint Blockade. Cell *178*, 933–948.e14. https://doi.org/10.1016/j.cell.2019.07.019.

9. Williams, J.B., Li, S., Higgs, E.F., Cabanov, A., Wang, X., Huang, H., and Gajewski, T.F. (2020). Tumor heterogeneity and clonal cooperation influence the immune selection of IFN-γ-signaling mutant cancer cells. Nat. Commun. *11*, 602. https://doi.org/10.1038/s41467-020-14290-4.

10. Dubrot, J., Du, P.P., Lane-Reticker, S.K., Kessler, E.A., Muscato, A.J., Mehta, A., Freeman, S.S., Allen, P.M., Olander, K.E., Ockerman, K.M., et al. (2022). In vivo CRISPR screens reveal the landscape of immune evasion pathways across cancer. Nat. Immunol. *23*, 1495–1506. https://doi.org/10.1038/s41590-022-01315-x.

Cancer Cell, Volume *41*

Supplemental information

Mutations in IFN-γ signaling genes sensitize tumors to immune checkpoint blockade

Eric Song and Ryan D. Chow

Figure S1

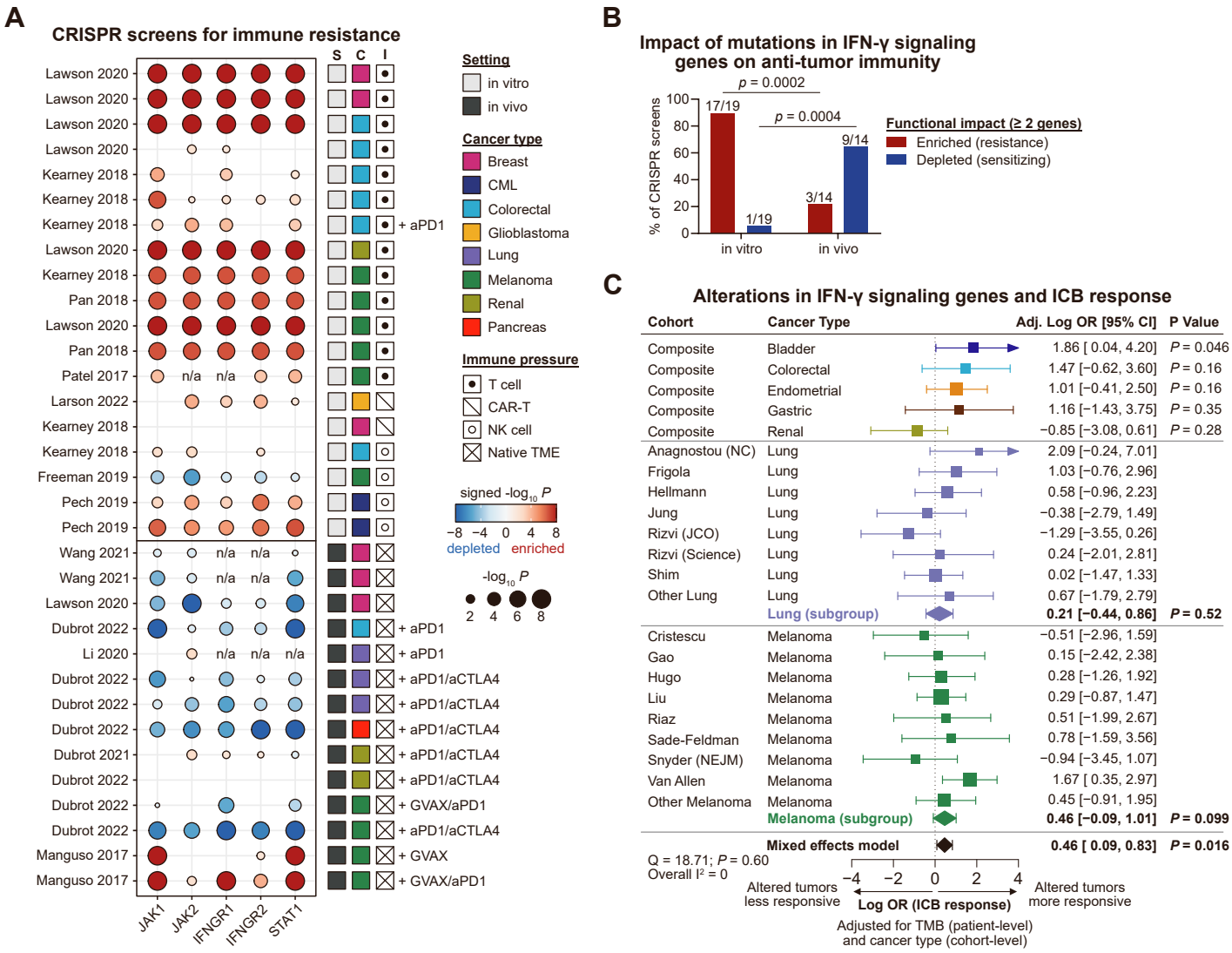

Figure S1: Mutations in IFN-γ signaling genes confer resistance to anti-tumor immunity *in vitro* but potentiate immune checkpoint blockade *in vivo*

A. Dot plot detailing the functional impact of mutations in *JAK1, JAK2, IFNGR1, IFNGR2,* or *STAT1* in the presence of anti-tumor immune pressure. Data shown are compiled from 33 CRISPR screens. Details regarding the experimental system in each screen are annotated to the right. Dots are scaled according to statistical significance and color-coded to indicate enrichment (red) or depletion (blue). Data points that did not meet the nominal significance threshold of $P < 0.05$ were omitted from the visualization.

B. Bar plot detailing the proportion of *in vitro* and *in vivo* CRISPR screens in which IFN-γ signaling gene alterations were significantly associated with resistance (red) or sensitivity (blue) to anti-tumor immunity. Statistical significance was assessed by two-tailed Fisher's exact test.

C. Mixed-effects meta-analysis of 2154 patients treated with ICB. Forest plot detailing the relation between pre-treatment alterations in IFN-γ signaling genes (*JAK1, JAK2, IFNGR1, IFNGR2,* or *STAT1*) and ICB response. Data are shown in terms of log odds ratios (ORs), adjusted for tumor mutation burden (TMB) at the patient-level and for tumor type at the cohort-level, with 95% confidence intervals. Symbol sizes are scaled according to study weight in the overall meta-analysis. Subgroup analyses for lung cancer and melanoma are also shown, along with Cochran's Q and I^2 heterogeneity metrics.

Supplemental Material

Data and code availability

- All datasets used in this study are available in the supplementary tables, Github (https://github.com/rdchow/IFNG_ICB), and Zenodo (https://zenodo.org/record/7534228, doi: 10.5281/zenodo.7534228)
- All custom analysis code is available on Github (https://github.com/rdchow/IFNG_ICB) and Zenodo (https://zenodo.org/record/7534228, doi: 10.5281/zenodo.7534228).
- Any additional information required to reanalyze the data reported in this work is available from the Lead Contact upon request.

Author contributions

E.S. compiled the datasets and secured funding. R.D.C. conceived and designed the study, conducted the analysis, and prepared the manuscript.

Methods

Construction of the clinicogenomic cohort

A final set of 2154 ICB-treated patients with tumor sequencing information were compiled from 29 studies. If multiple tissues were represented in a single dataset, the study cohort was split by tissue type. The sources of the relevant genomic and clinical data from each of these studies are detailed below, and the processed patient-level data are provided in the supplementary tables, Github (https://github.com/rdchow/IFNG_ICB) and Zenodo (https://zenodo.org/record/7534228).

A limitation of our analysis is that an unknown proportion of the identified missense IFN-γ signaling gene alterations are functionally neutral ("benign"). In the absence of detailed experimental characterizations for each possible mutation, for our primary analysis we sought to undertake an unbiased survey of these alterations and thus included all missense mutations. As a secondary analysis, we also cross-referenced all variants with the OncoKB database and further used the ESM1b (ref #5 in main text) or EVE (ref #6 in main text) pathogenicity prediction algorithms to classify "pathogenic" vs "benign" missense mutations. We then repeated the analyses after excluding samples with predicted benign missense mutations (ESM1b and/or EVE) or putative gain-of-function alterations (as annotated in OncoKB) in IFN-γ signaling genes. In our cohort, one *JAK1* variant (p.G1097D) was annotated in OncoKB as likely gain-of-function; this

sample was therefore classified as unaltered and excluded for the secondary analysis, as our intention was to investigate the consequences of IFN-γ signaling loss (rather than gain). An ESM1b threshold of ≤ -7.5 was chosen to define predicted pathogenic mutations, while we used the "EVE_classes_75_pct_retained_ASM" pathogenicity classification from EVE. In situations where the specific nonsynonymous amino acid change was not annotated or could not be otherwise determined from the available data, we retained these variants by default in the interest of maintaining sensitivity. *JAK1* pathogenicity prediction scores were not available from the precomputed EVE database; thus, all *JAK1* missense variants were scored as predicted pathogenic in the EVE-based analysis. In Table S1, the ESM1b and EVE pathogenicity scores are annotated for each missense variant as "AminoAcidChange: ESM1b_score | EVE_score."

Data sources for ICB-treated patient cohorts

We apologize to the authors of the studies noted here that we were unable to cite in the main reference list. The 15 studies cited in the supplemental references were selected using a random number generator on the CRISPR screens or ICB clinicogenomic cohorts included in our study. All supplemental references can be found on Github (https://github.com/rdchow/IFNG_ICB/blob/main/supplementary-references-all.txt).

Anagnostou et al, Nature Cancer 2020 [1]

This cohort was profiled by whole-exome sequencing. All clinical and genomic data were acquired from the supplementary tables. Treatment response information was not provided in terms of best RECIST objective response, so the authors' classifications of "durable clinical benefit" vs "no durable benefit" were used instead. Non-synonymous variants in *JAK1*, *JAK2*, *IFNGR1*, *IFNGR2*, and *STAT1* were collated. TMB was based on the total number of non-synonymous variants in the provided variant calls for each sample.

Anagnostou et al, Cell Reports Medicine 2020

This cohort was profiled by whole-exome sequencing. All clinical and genomic data were acquired from the supplementary tables. Treatment response information was binarized into non-responders (SD, PD) or responders (PR, CR) based on the provided best objective response information. Non-synonymous variants in *JAK1*, *JAK2*, *IFNGR1*, *IFNGR2*, and *STAT1* were

collated. TMB was based on the total number of non-synonymous variants in the provided variant calls for each sample.

Braun et al, Nature Medicine 2020

This cohort was profiled by whole-exome sequencing. All clinical and genomic data were acquired from the supplementary tables, including TMB values. Treatment response information was binarized into non-responders (SD, PD) or responders (PR, CR) based on the provided best objective response information. Non-synonymous variants in *JAK1*, *JAK2*, *IFNGR1*, *IFNGR2*, and *STAT1* were collated.

Chow et al, Cancer Discovery 2022 (ref #4 in main text)

This cohort was profiled by whole-exome sequencing. All clinical and genomic data were acquired from the supplementary tables, including TMB values. Treatment response information was binarized into non-responders (SD, PD) or responders (PR, CR) based on the provided best objective response information. Non-synonymous variants in *JAK1*, *JAK2*, *IFNGR1*, *IFNGR2*, and *STAT1* were collated.

Cristescu, Science 2018

This cohort was profiled by whole-exome sequencing. As the genomic and clinical response information were not provided in the supplementary tables, best objective response information, TMB, and alteration status of *JAK1* and *JAK2* were instead obtained from Litchfield et al.[2] The dataset was then split by cancer type for further analysis.

Frigola et al, Mol Oncol 2021

This cohort was profiled by whole-exome sequencing. All clinical and genomic data were acquired from the supplementary tables. Treatment response information was binarized into non-responders (SD, PD) or responder (PR, CR) based on the provided best objective response information. Non-synonymous variants in *JAK1*, *JAK2*, *IFNGR1*, *IFNGR2*, and *STAT1* were collated. TMB was calculated based on the total number of non-synonymous variants in the provided variant calls for each sample.

Gao et al, Cell 2016 (ref #2 in main text)

This cohort was profiled by whole-exome sequencing. The variant calls were not available in the supplementary tables, so variants and deletions in *JAK1*, *JAK2*, *IFNGR1*, and *IFNGR2* were collated from Figure 1. *STAT1* alterations were not represented in the figures, and thus we could not include *STAT1* in our assessment. Treatment response information was binarized into non-responders and responders. TMB information was not publicly available for this cohort.

Hellmann et al, Cancer Cell 2018

This cohort was profiled by whole-exome sequencing. The variant calls were accessed on cBioPortal (https://www.cbioportal.org/study/summary?id=nsclc_mskcc_2018), querying for mutations in *JAK1*, *JAK2*, *IFNGR1*, *IFNGR2*, and *STAT1*. Treatment response information was binarized into non-responders (SD, PD) or responder (PR, CR) based on the provided best objective response information. TMB values were taken from the cBioPortal dataset.

Hugo et al, Cell 2016 [3]

This cohort was profiled by whole-exome sequencing. The variant calls were accessed on cBioPortal (https://www.cbioportal.org/study/summary?id=mel_ucla_2016), querying for mutations or homozygous deletions in *JAK1*, *JAK2*, *IFNGR1*, *IFNGR2*, and *STAT1*. Treatment response information was binarized into non-responders (SD, PD) or responder (PR, CR) based on the provided best objective response information. TMB values were taken from the cBioPortal dataset.

Jung et al, Nature Communications 2019

This cohort was profiled by whole-exome sequencing. All clinical and genomic data were acquired from the supplementary tables, including TMB values. Treatment response information was not provided in terms of best RECIST objective response, so the authors' classifications of "durable clinical benefit" vs "no durable benefit" were used instead. Non-synonymous variants in *JAK1*, *JAK2*, *IFNGR1*, *IFNGR2*, and *STAT1* were collated.

Kim et al, Nature Medicine 2018

This cohort was profiled by whole-exome sequencing. The clinical and genomic data were not available from the supplementary tables or on cBioportal. Instead, these data were collected from Zenodo (https://zenodo.org/record/7044234), associated with a reanalysis by Bareche et al.[4] Non-synonymous variants in *JAK1*, *JAK2*, *IFNGR1*, *IFNGR2*, and *STAT1* were collated. Response status was determined from the authors' designations. TMB was determined by counting the number of nonsynonymous mutations in each sample.

Le et al, New England Journal of Medicine 2015

This cohort was profiled by whole-exome sequencing. As the genomic data were not provided in the supplementary tables, alteration status of *JAK1* and *JAK2* was instead obtained from Litchfield et al. Clinical response information by RECIST and TMB values were also determined from the Litchfield dataset.

Liu et al, Nature Medicine 2019

This cohort was profiled by whole-exome sequencing. All clinical and genomic data were found on cBioPortal (https://www.cbioportal.org/study/summary?id=mel_dfci_2019). Treatment response information was binarized into non-responders (SD, PD) or responder (PR, CR) based on the provided best objective response information. Non-synonymous variants and homozygous deletions in *JAK1*, *JAK2*, *IFNGR1*, *IFNGR2*, and *STAT1* were collated. TMB values were taken from the cBioPortal dataset.

Mariathasan et al, Nature 2018 [5]

This cohort was profiled by whole-exome sequencing. All clinical and genomic data (including TMB values) were collected from the authors' R package IMvigor210CoreBiologies (http://research-pub.gene.com/IMvigor210CoreBiologies/). Non-synonymous variants in *JAK1* and *JAK2* were collated; mutations in the other 3 genes were not present in the provided dataset.

McDermott et al, Nature Medicine 2018

This cohort was profiled by whole-exome sequencing. As the clinical and genomic data were not provided in the supplementary tables, response information, TMB values, and alteration status of *JAK1* and *JAK2* were instead obtained from Litchfield et al.

Miao et al, Nature Genetics 2018 [6]

This cohort was profiled by whole-exome sequencing. Clinical and genomic data were found on cBioPortal (https://www.cbioportal.org/study/summary?id=mixed_allen_2018). Treatment response information was binarized into non-responders (SD, PD) or responder (PR, CR) based on the provided best objective response information. Non-synonymous variants in *JAK1*, *JAK2*, *IFNGR1*, *IFNGR2*, and *STAT1* were collated. TMB values were taken from the cBioPortal dataset. Since this cohort included re-analyses of previously published cohorts, we removed all duplicate samples that were already included elsewhere in our study (namely the Van Allen Science 2015, Snyder NEJM 2014, and Rizvi Science 2015 cohorts).

Miao et al, Science 2018

This cohort was profiled by whole-exome sequencing. All clinical and genomic data were found on cBioPortal (https://www.cbioportal.org/study/summary?id=ccrcc_dfci_2019). TMB values were taken from the cBioPortal dataset. Treatment response information was binarized into non-responders (SD, PD) or responder (PR, CR) based on the provided best objective response information. Non-synonymous variants and homozygous deletions in *JAK1*, *JAK2*, *IFNGR1*, *IFNGR2*, and *STAT1* were collated.

Nathanson et al, Cancer Immunol Res 2017

This cohort was profiled by whole-exome sequencing. All clinical and genomic data were found online from http://www.hammerlab.org/melanoma-reanalysis/. All SNVs and indels in *JAK1*, *JAK2*, *IFNGR1*, *IFNGR2*, and *STAT1* were collated. Treatment response information was not provided in terms of best RECIST objective response, so the authors' classifications of "durable clinical benefit" vs "no durable benefit" were used instead. TMB was determined by counting the number of nonsynonymous mutations in each sample.

Pleasance et al, Nature Cancer 2020

This cohort was profiled by whole-exome sequencing. Clinical and genomic data were on cBioPortal (https://www.cbioportal.org/study/summary?id=pog570_bcgsc_2020). Non-

synonymous variants and homozygous deletions in *JAK1*, *JAK2*, *IFNGR1*, *IFNGR2*, and *STAT1* were collated. TMB values were taken from the cBioPortal dataset.

Riaz et al, Cell 2017 [7]

This cohort was profiled by whole-exome sequencing. All clinical and genomic data were acquired from the supplementary tables, including TMB. Treatment response information was binarized into non-responders (SD, PD) or responder (PR, CR) based on the provided best objective response information. Non-synonymous variants in *JAK1*, *JAK2*, *IFNGR1*, *IFNGR2*, and *STAT1* were collated.

Rizvi et al, Science 2015

This cohort was profiled by whole-exome sequencing. Clinical and genomic data were on cBioPortal (https://www.cbioportal.org/study/summary?id=luad_mskcc_2015). Non-synonymous variants in *JAK1*, *JAK2*, and *IFNGR1* were collated. Treatment response information was binarized into non-responders (SD, PD) or responder (PR, CR) based on the provided best objective response information. TMB values were taken from the cBioPortal dataset.

Rizvi et al, Journal of Clinical Oncology 2018

This cohort was profiled by targeted NGS (MSK-IMPACT). Clinical and genomic data were on cBioPortal (https://www.cbioportal.org/study/summary?id=luad_mskcc_2015). Non-synonymous variants in *JAK1*, *JAK2*, *IFNGR1*, *IFNGR2*, and *STAT1* were collated. TMB values were taken from the cBioPortal dataset. Treatment response information was not provided in terms of best RECIST objective response, so the authors' classifications of "durable clinical benefit" vs "no durable benefit" were used instead.

Roh et al, Science Translational Medicine 2017 [8]

This cohort was profiled by whole-exome sequencing. All clinical and genomic data were acquired from the supplementary tables. Treatment response information was binarized into non-responders or responder based on the authors' assessment; patients with a response to either CTLA-4 or PD-1 therapy were classified as responders. Non-synonymous variants in *JAK1*, *JAK2*,

IFNGR1, *IFNGR2*, and *STAT1* were collated. TMB was determined by counting the number of nonsynonymous mutations in each sample.

Sade-Feldman et al, Nature Communications 2017

This cohort was profiled by whole-exome sequencing. The variant calls were not available in the supplementary tables, so variants and deletions in *JAK1*, *JAK2*, *IFNGR1*, *IFNGR2*, and *STAT1* were collated from Figure S7 in the publication. Treatment response information was binarized into non-responders and responders, labeling "resistance" samples as responders (as these tumors had initially responded). Only patients with pre-treatment tumors were considered. TMB values were reconstructed from Figure S7 using WebPlotDigitizer (https://apps.automeris.io/wpd/).

Shim et al, Ann Oncology 2020

This cohort was profiled by whole-exome sequencing. The clinical and genomic data were not available, so we referred to Figure S4 in the publication to determine *JAK1* and *JAK2* alteration status, along with clinical response classifications and TMB values. TMB values were reconstructed from Figure S4 using WebPlotDigitizer (https://apps.automeris.io/wpd/).

Snyder et al, New England Journal of Medicine 2014 [9]

This cohort was profiled by whole-exome sequencing. Clinical and genomic data were on cBioPortal (https://www.cbioportal.org/study/summary?id=skcm_mskcc_2014). Non-synonymous variants and homozygous deletions in *JAK1*, *JAK2*, *IFNGR1*, *IFNGR2*, and *STAT1* were collated. Treatment response information was binarized into non-responders and responders, as determined by the authors. TMB values were taken from the cBioPortal dataset.

Snyder et al, PLOS Medicine 2017

This cohort was profiled by whole-exome sequencing. Clinical and genomic data were on Zenodo (https://zenodo.org/record/546110) and Github (https://github.com/hammerlab/multi-omic-urothelial-anti-pdl1), including the number of nonsynonymous variants in each sample. Variant effects were manually reviewed and translated to determine non-silent variants *JAK1*, *JAK2*, *IFNGR1*, *IFNGR2*, and *STAT1*. Treatment response information was binarized into non-

responders (SD, PD) or responder (PR, CR) based on the provided best objective response information.

Van Allen et al, Science 2015 [10]

This cohort was profiled by whole-exome sequencing. Clinical and genomic data were on cBioPortal (https://www.cbioportal.org/study/summary?id=skcm_dfci_2015). Non-synonymous variants and homozygous deletions in *JAK1*, *JAK2*, *IFNGR1*, *IFNGR2*, and *STAT1* were collated. Treatment response information was binarized into non-responders (SD, PD) or responder (PR, CR) based on the provided best objective response information. TMB values were taken from the cBioPortal dataset.

Yang et al, Nature Communications 2021 [11]

This cohort was profiled by whole-exome sequencing. The clinical and genomic data were not available from the supplementary tables or on cBioportal. Instead, these data were collected from Zenodo (https://zenodo.org/record/7044234), associated with a reanalysis by Bareche et al.[4] Non-synonymous variants in *JAK1*, *JAK2*, *IFNGR1*, *IFNGR2*, and *STAT1* were collated. Treatment response information was binarized into non-responders (SD, PD) or responder (PR, CR) based on the provided best objective response information. TMB values were determined based on the number of nonsynonymous variants.

Cohort filtering and merging

For our final analysis, we excluded all patients whose tumors were profiled only after initiating ICB treatment. Patients who were not evaluable for ICB response were also excluded. Our approach to cohort filtering and merging was designed to minimize the number of cohorts containing 0 counts, and to maximize the number of informative cohorts. The two criteria for keeping a cohort as-is without merging were as follows:

Criteria A: If a cohort has ≥ 15 patients AND ≥ 4 altered samples (regardless of 0 counts)

Criteria B: If a cohort has ≥ 2 altered samples, ≥ 15 patients, and no 0 counts

For the remaining studies/cohorts of a given tissue type (if < 2 altered samples OR < 15 patients OR ≥ 1 category with a 0 count), the following steps were utilized to filter and/or merge cohorts.

1. Aggregate together the remaining studies of a given cancer type.
2. If the aggregated cohort now meets either Criteria A or B, keep it as a merged/composite cohort and stop.
3. If the aggregated cohort still does not meet those criteria, then merge it with the next smallest study of that cancer type that had individually passed met either Criteria A or B (if any).
4. Repeat step 3 until the merged cohort passes either Criteria A or B.
5. If there are no more studies from a given cancer type to aggregate with, and Criteria A or B were still not met, stop and remove this cancer type entirely from further analysis.

The detailed patient-level annotations are shown in Table S1, including patients that were eventually excluded from the final analysis. The breast cancer cohort was ultimately excluded from the multi-level mixed-effects meta-analysis due to issues with model convergence. As noted above, we also conducted a sensitivity analysis where we the repeated the above process after excluding patients with missense mutations that were scored as benign based on ESM1b or EVE pathogenicity scores or annotated as gain-of-function on the OncoKB database.

Meta-analysis of the ICB-treated patient cohort

We used Firth's penalized likelihood logistic regression to estimate the effect size for IFN-γ alterations on ICB response within each cohort, simultaneously accounting for TMB as a covariate. TMB was binarized by the median TMB value within each cohort. For cohorts that represented a composite of multiple studies (7 of 22 final cohorts), TMB was not included in the regression model, as the experimental platforms and statistical methods used to calculate TMB varied across studies. In addition, one cohort (Gao Melanoma) did not have readily available TMB values.

We then conducted a weighted multi-level mixed effects meta-analysis in R (4.0.2) with the *rma.mv* function from the metafor package, incorporating an additional layer for cancer type. The restricted maximum likelihood estimator was used. Results were visualized as a forest plot, detailing the natural log-transformed adjusted odds ratios. Heterogeneity was assessed by Cochran's Q test and by I^2 metrics.

Analysis of CRISPR genetic screens

We apologize to the authors of the studies noted here that we were unable to cite in the main reference list. The 15 studies cited in the supplemental references were selected using a random number generator on the CRISPR screens or ICB clinicogenomic cohorts included in our study. All supplemental references can be found on Github (https://github.com/rdchow/IFNG_ICB/blob/main/supplementary-references-all.txt).

In total, 33 different CRISPR screens were collected from 12 published studies. The pertinent experimental details and statistical approaches employed in each of these studies are summarized below, using the authors' own phrasing where applicable. For the purpose of determining whether IFN-γ signaling gene alterations were enriched or depleted in the presence of immune pressure, we set a threshold of ≥ 2 significantly enriched/depleted genes. This threshold was selected for two reasons: 1) in CRISPR screens, having multiple enriched/depleted genes in the same pathway is more indicative of a true pathway-level effect, and 2) several of the included screens did not target all 5 genes in the CRISPR library.

Dubrot et al, Immunity 2021 [12]

- Tumor cell target: Renca renal cell carcinoma cells, implanted subcutaneously into NSG or WT mice. (in vivo)
- sgRNA library: "9,672 sgRNAs targeting 2,368 genes with 4 guides per gene along with non-targeting control guides (described in (Manguso et al., 2017)). Briefly, this library targeted genes that were enriched in the Gene Ontology (GO) term categories kinase, phosphatase, cell surface, plasma membrane, antigen processing and presentation, immune system process, and chromatin remodeling, and that were expressed in B16 melanoma."
- Immune pressure: The WT mice had an intact immune system compared to NSG mice. The WT mice also received 100ug anti-PD1 + 100ug anti-CTLA-4.
- Analysis: "A z-score normalization was applied before comparing guide abundances between conditions. One guide was removed from analysis due to aberrantly high abundance in the input. Hit calling and statistical significance for sgRNA enrichment or depletion between groups was determined using the STARS algorithm (Doench et al., 2014)."

Dubrot et al, Nature Immunology 2022 (ref #10 in main text)

- Tumor cell target: B16 melanoma, CT26 colorectal cancer, KPC lung adenocarcinoma LLC Lewis lung carcinoma, MC38 colorectal cancer, Panc02 pancreatic adenocarcinoma, Renca renal cell carcinoma, YUMMER melanoma, all transplanted into NSG vs WT mice treated with ICB. (in vivo)
- sgRNA library: "For the genome-scale in vivo screens, a library of 18,748 genes, each targeted by four sgRNAs delivered in four separate cohorts (Brie Library)."
- Immune pressure: The WT mice had an intact immune system compared to NSG mice. The WT mice also received ICB therapies, depending on the specific tumor type being investigated.
- Analysis: "Read counts were library normalized per 1 million reads and log2 transformed with a pseudocount of one. Gene-targeting guides were z normalized by the control sgRNA distribution. Guide fold changes were calculated as residuals fit to a natural cubic spline with 4 d.f. For the genome-scale screens, fold changes from all four pools were quantile normalized with gene-wise mean imputation before downstream analyses. Enriched and depleted genes for each screen were calculated using the STARS algorithm"

Freeman et al, Cell Reports 2019

- Tumor cell target: B16-F10 murine melanoma cells, expressing OVA. (in vitro)
- sgRNA library: Brie genome-wide sgRNA library
- Immune pressure: Primary NK cells isolated from female C57BL/6 splenocytes. "Brie-transduced B16-F10 Cas9 tumor cells were co-cultured with NK cells at a 1:1 E:T ratio overnight in technical duplicate determinations. Tumor cells were allowed sufficient time to recover before being subjected to another round of NK co-culture; this process was repeated for a total of 3 NK co-cultures."
- Analysis: "Model-based Analysis of Genome-wide CRISPR/Cas9 Knockout, v0.5.7 (MAGeCK count and MAGeCK test) software was subsequently used to count the reads and perform gene/sgRNA enrichment/depletion and statistical analyses between treated/sorted and control samples (Li et al., 2014)."

Kearney et al, Science Immunology 2018

- Tumor cell target: MC38 and B16 cell lines expressing OVA, or MDA-MB-231 cells. (in vitro)
- sgRNA library: Brie genome-wide sgRNA library, or Brunello genome-wide library for MDA-MB-231 cells.
- Immune pressure: "OT-I T cells from wild-type mice were activated from spleens with the chicken Ova peptide SIINFEKL. Activated T cells were used on days 5 to 10 and had a typical effector phenotype (CD8+CD69+CD25+CD62L−CD44+)." NK cells were also isolated from wild-type mice.
- Analysis: "MAGeCK (v0.5.6) was used to count the reads and perform gene/sgRNA enrichment and statistical analysis."

Lawson et al, Nature 2020 [13]

- Tumor cell target: Renca, CT26, B16, MC38, 4T1 and EMT6, expressing HA or Ova. (in vitro). EMT6 expressing HA transplanted in BALB/c vs NCG mice. (in vivo)
- sgRNA library: "An optimized Streptococcus pyogenes Cas9 (spCas9) guide RNA (gRNA) library containing 94,528 gRNAs that target 19,069 protein-coding genes. We then used this library (which we call the mouse Toronto KnockOut, or mTKO, library)."
- Immune pressure: "For T cell killing screens, the experimental groups were treated with preactivated CL4 or OT-1 CD8+ T cells to achieve approximately 50% or higher cytotoxicity (determined by microscopic evaluation), with control groups being treated with wild-type CD8+ T cells (B16–Ova, MC38–Ova) or left untreated (Renca–HA, EMT6–HA, 4T1–HA, CT26–HA). Treatments were repeated 2–3 times throughout the course of each screen."
- Analysis: "Read counts for all samples in a screen were combined in a matrix and normalized to 10 million reads per sample by dividing each read count by the sum of all read counts in the sample and then multiplying by 10 million. Fold change is calculated against a reference sample (usually T0). Bayes Factor (BF) scores were calculated as previously described" using DrugZ.

Larson et al, Nature 2022 [14]

- Tumor cell target: U87 glioblastoma cell line. (in vitro)
- sgRNA library: Brunello human genome-wide library
- Immune pressure: Anti-EGFR CAR-Ts (cetuximab), "with a CD8 hinge and transmembrane domain (except CD28 CAR constructs, which have a CD28 hinge and transmembrane domain), 4-1BB costimulatory domain (unless otherwise stated as CD28), CD3ζ signalling domain, and fluorescent reporter mCherry to evaluate transduction efficiency."
- Analysis: "Read count matrices for each sgRNA barcode and sample were quantified using PoolQ version 3.2.10. Counts were aggregated summed across lanes and technical replicates." Since the gene-level analyses were not provided by the authors in the supplementary tables, but the gene count matrices were provided, we performed a re-analysis using MAGeCK, specifying the non-targeting control sgRNA set in the Brunello library as a control.

Li et al, Cancer Discovery 2020

- Tumor cell target: KP (Kras-G12D, p53 KO) lung cancer cell line from pure C57BL/6 mice, transplanted subcutaneously. (in vivo)
- sgRNA library: "The library contains 7,780 sgRNAs, including sgRNAs targeting 524 epigenetic regulators, 173 control genes (essential genes, immune modulators, etc.), and 723 nontargeting sgRNAs. For each gene, there are 8 to 12 sgRNAs. Additional details of the library are included in Supplementary Table S1."
- Immune pressure: "KP-Cas9 clones with validated Cas9 activity were transduced at a MOI of 0.2 with lentivirus produced from the libraries with at least 1,000-fold coverage (cells per construct) in each infection replicate. Transduced KP cells were expanded in vitro for 2 weeks and then subcutaneously implanted into B6-Rag1−/− mice and C57BL/6 mice. These mice were then treated with anti–PD-1 or isotype control (3 times per week) on day 7 when the average tumor size reached 60 mm3; tumors were harvested on day 24 when the tumor size was roughly 500 mm3."
- Analysis: "The count tables were normalized based on their library size factors using DESeq2, and differential expression analysis was performed. Further, MAGeCK (0.5.8)

was used to normalize the count table based on median normalization and fold changes, and significance of changes in the conditions was calculated for genes and sgRNAs."

Manguso et al, Nature 2017

- Tumor cell target: B16 melanoma cells, transplanted subcutaneously into mice. (in vivo)
- sgRNA library: "9,992 optimized sgRNAs targeting 2,398 genes, which were selected from the Gene Ontology (GO) term categories: kinase, phosphatase, cell surface, plasma membrane, antigen processing and presentation, immune system process, and chromatin remodelling. The transcript abundance of the genes in these categories were then filtered to include only those that were expressed >RPKM(log2) = 0.9. These genes were then ranked for expression in the B16 cell line using RNA-sequencing to select for the top 2,398 expressed genes."
- Immune pressure: "B16 cells were implanted into 10 Tcra−/− mice, 10 wild-type mice treated with GVAX, and 10 wild-type mice treated with GVAX and PD-1 blockade. B16 cells transduced with libraries were also grown in vitro at approximately 2,000× library coverage for the same time period as the animal experiment. Mice were euthanized 12–14 days after tumour implantation."
- Analysis: "Significantly enriched or depleted sgRNAs from any comparison of conditions were identified using the STARS algorithm."

Pan et al, Science 2018

- Tumor cell target: B16F10 melanoma cells. (in vitro)
- sgRNA library: Brie murine genome-wide sgRNA library
- Immune pressure: "Pmel-1 and OT-I TCR transgenic mice were purchased from Jackson Laboratory (stock # 005023 for Pmel-1 and 003831 for OT-1). CD8 T cells were isolated from spleen and lymph nodes from Pmel-1 or OT-I TCR transgenic mice. B16F10 cells were pretreated with 10ng/ml of IFNg for 24 hours prior to co-culture with Pmel-1 T cells to increase MHC class I expression. For the OT-I screen, B16F10 cells were pulsed with 1ng/ml of Ova peptide (SIINFEKL) at 37oC for 2 hours prior to co-culture with OT-I T cells. Given that killing of tumor cells by OT-I was rapid, B16F10 and OT-I T cells were co-cultured for one day before T cells were removed from the culture. Genomic DNA was

extracted from cells regrown following T cell removal, and the gRNA cassette was sequenced as described above."

- Analysis: "For candidate gene discovery, the normalized gRNA count table was loaded into MaGeCK (Model-based Analysis of Genome-wide CRISPR-Cas9 Knockout) by comparing the experimental and control conditions described above. Top genes were determined based on mean log2 fold change (LFC) for all gRNAs and false discovery rate (FDR)."

Patel et al, Nature 2017

- Tumor cell target: "The melanoma cell lines HLA-A*02+/MART-1+/NY-ESO-1+ (Mel624.38, Mel1300), HLA-A*02− (Mel938) and HLA-A*02+/NY-ESO-1− (Mel526) were isolated from surgically resected metastases." (in vitro)
- sgRNA library: GeCKOv.2 murine genome-wide sgRNA library.
- Immune pressure: "Cell–cell interaction genome-wide screens were performed using Mel624 cells transduced independently with both A and B GeCKOv.2 libraries. For one screen, we split two groups of 5×10^7 transduced Mel624 cells. One group was co-cultured with 1.67×10^7 patient-derived NY-ESO-1 T cells (E:T ratio of 1:3 or 0.3) for each library. A second (control) group were cultured under the same density and conditions but without T cells. The co-culture phase was maintained for 12 h after which the T cells were removed as described above. The recovery phase was maintained for another 48 h.
- Analysis: "Counts were normalized by the total reads for each sample and then log-transformed. A gene ranking was computed using the second-most-enriched sgRNA for each gene (second-most-enriched sgRNA score) and the RIGER weighted-sum method."

Pech et al, eLife 2019

- Tumor cell target: K562 leukemia cells. (in vitro)
- sgRNA library: "The sgRNA library was designed with 120,021 sgRNAs present, representing six guides each against 21,598 genes and four guides each against 1918 miRNAs, as well as 1000 non-targeting negative control guides (Supplementary file 1). sgRNAs targeting protein-coding genes were based on the Avana libraries (Doench et al., 2016)."

- Immune pressure: NK92 human NK cell line. “Seven days post guide-infection, NK cell challenge was initiated. For the 2.5:1 E:T challenge, 100M K562 cells were mixed with 250M NK-92 cells in 1L of Myelocult, and split across 25 177 cm2 dishes. For the 1:1 E:T challenge, 100M K562 cells were mixed with 100M NK-92 cells in 400mls of Myelocult, and split across 10 177 cm2 dishes. As a control, K562 cells were continuously propagated in RPMI media.
- Analysis: “Protospacer count tables were generated from these alignments with python scripts and processed with MAGeCK. MAGeCK analysis was used to score and prioritize sgRNAs, using default settings in the algorithm (Li et al., 2014). A subset of genes, mostly from highly related gene families, have more than six sgRNAs targeting them. As the MAGeCK scoring method tends to prioritize consistency of effect over magnitude of effect, genes with more than six guides targeting them were excluded from the analysis. MAGeCK scores were -log10 normalized, and values were plotted against FDR values.”

Wang et al, Cell 2021 [15]

- Tumor cell target: Murine 4T1, EMT6, JC breast cancer cells, transplanted into mice. (in vivo)
- sgRNA library: “The MusCK library consisted of 24,622 sgRNAs including 1,000 non-targeting controls (NTCs) and 23,622 unique sgRNAs targeting 4,787 gene locations in the genome. The MusCK 2.0 library consisted of 800 sgRNAs including 168 non-targeting controls (NTCs) and 632 unique sgRNAs targeting 79 gene locations in the genome. In the MusCK 2.0 library, eight sgRNAs (four designed by our group in MusCK, another four referenced from the Broad Institute’s Brie Mouse CRISPR Knockout Pool Library) (Doench et al., 2016) were designated to each candidate gene.”
- Immune pressure: “Transduced murine cancer cells were expanded in vitro for 1 week to allow genome editing before being implanted into animals. Cancer cells were either injected into the mammary fat pads of mice or subcutaneously with Matrigel (1:1 dilution). Cancer cells were implanted into both flanks of 10-12 Foxn1nu/nu mice, 10-12 wild-type mice, 10-12 wild-type mice treated with ovalbumin, and 10-12 wild-type mice treated with ovalbumin and PD-1 blockade. Mice were vaccinated with ovalbumin twice (once a week) 14 days before cancer cell transplantation.”

- Analysis: “Significantly enriched or depleted sgRNAs from any comparison of conditions were identified using the MAGeCK algorithm.”

Supplemental References

1. Anagnostou, V., Niknafs, N., Marrone, K., Bruhm, D.C., White, J.R., Naidoo, J., Hummelink, K., Monkhorst, K., Lalezari, F., Lanis, M., et al. (2020). Multimodal genomic features predict outcome of immune checkpoint blockade in non-small-cell lung cancer. Nat Cancer *1*, 99–111. 10.1038/s43018-019-0008-8.

2. Litchfield, K., Reading, J.L., Puttick, C., Thakkar, K., Abbosh, C., Bentham, R., Watkins, T.B.K., Rosenthal, R., Biswas, D., Rowan, A., et al. (2021). Meta-analysis of tumor- and T cell-intrinsic mechanisms of sensitization to checkpoint inhibition. Cell *184*, 596-614.e14. 10.1016/j.cell.2021.01.002.

3. Hugo, W., Zaretsky, J.M., Sun, L., Song, C., Moreno, B.H., Hu-Lieskovan, S., Berent-Maoz, B., Pang, J., Chmielowski, B., Cherry, G., et al. (2016). Genomic and Transcriptomic Features of Response to Anti-PD-1 Therapy in Metastatic Melanoma. Cell *165*, 35–44. 10.1016/j.cell.2016.02.065.

4. Bareche, Y., Kelly, D., Abbas-Aghababazadeh, F., Nakano, M., Esfahani, P.N., Tkachuk, D., Mohammad, H., Samstein, R., Lee, C.-H., Morris, L.G.T., et al. (2022). Leveraging Big Data of Immune Checkpoint Blockade Response Identifies Novel Potential Targets. Annals of Oncology *0*. 10.1016/j.annonc.2022.08.084.

5. Mariathasan, S., Turley, S.J., Nickles, D., Castiglioni, A., Yuen, K., Wang, Y., Kadel, E.E., Koeppen, H., Astarita, J.L., Cubas, R., et al. (2018). TGFβ attenuates tumour response to PD-L1 blockade by contributing to exclusion of T cells. Nature *554*, 544–548. 10.1038/nature25501.

6. Miao, D., Margolis, C.A., Vokes, N.I., Liu, D., Taylor-Weiner, A., Wankowicz, S.M., Adeegbe, D., Keliher, D., Schilling, B., Tracy, A., et al. (2018). Genomic correlates of response to immune checkpoint blockade in microsatellite-stable solid tumors. Nat Genet *50*, 1271–1281. 10.1038/s41588-018-0200-2.

7. Riaz, N., Havel, J.J., Makarov, V., Desrichard, A., Urba, W.J., Sims, J.S., Hodi, F.S., Martín-Algarra, S., Mandal, R., Sharfman, W.H., et al. (2017). Tumor and Microenvironment Evolution during Immunotherapy with Nivolumab. Cell *171*, 934-949.e16. 10.1016/j.cell.2017.09.028.

8. Roh, W., Chen, P.-L., Reuben, A., Spencer, C.N., Prieto, P.A., Miller, J.P., Gopalakrishnan, V., Wang, F., Cooper, Z.A., Reddy, S.M., et al. (2017). Integrated molecular analysis of tumor biopsies on sequential CTLA-4 and PD-1 blockade reveals markers of response and resistance. Science Translational Medicine *9*, eaah3560. 10.1126/scitranslmed.aah3560.

9. Snyder, A., Makarov, V., Merghoub, T., Yuan, J., Zaretsky, J.M., Desrichard, A., Walsh, L.A., Postow, M.A., Wong, P., Ho, T.S., et al. (2014). Genetic Basis for Clinical Response to CTLA-4 Blockade in Melanoma. New England Journal of Medicine *371*, 2189–2199. 10.1056/NEJMoa1406498.

10. Van Allen, E.M., Miao, D., Schilling, B., Shukla, S.A., Blank, C., Zimmer, L., Sucker, A., Hillen, U., Foppen, M.H.G., Goldinger, S.M., et al. (2015). Genomic correlates of response to CTLA-4 blockade in metastatic melanoma. Science *350*, 207–211. 10.1126/science.aad0095.

11. Cindy Yang, S.Y., Lien, S.C., Wang, B.X., Clouthier, D.L., Hanna, Y., Cirlan, I., Zhu, K., Bruce, J.P., El Ghamrasni, S., Iafolla, M.A.J., et al. (2021). Pan-cancer analysis of longitudinal metastatic tumors reveals genomic alterations and immune landscape dynamics associated with pembrolizumab sensitivity. Nat Commun *12*, 5137. 10.1038/s41467-021-25432-7.

12. Dubrot, J., Lane-Reticker, S.K., Kessler, E.A., Ayer, A., Mishra, G., Wolfe, C.H., Zimmer, M.D., Du, P.P., Mahapatra, A., Ockerman, K.M., et al. (2021). In vivo screens using a selective CRISPR antigen removal lentiviral vector system reveal immune dependencies in renal cell carcinoma. Immunity *54*, 571-585.e6. 10.1016/j.immuni.2021.01.001.

13. Lawson, K.A., Sousa, C.M., Zhang, X., Kim, E., Akthar, R., Caumanns, J.J., Yao, Y., Mikolajewicz, N., Ross, C., Brown, K.R., et al. (2020). Functional genomic landscape of cancer-intrinsic evasion of killing by T cells. Nature *586*, 120–126. 10.1038/s41586-020-2746-2.

14. Larson, R.C., Kann, M.C., Bailey, S.R., Haradhvala, N.J., Llopis, P.M., Bouffard, A.A., Scarfó, I., Leick, M.B., Grauwet, K., Berger, T.R., et al. (2022). CAR T cell killing requires the IFNγR pathway in solid but not liquid tumours. Nature *604*, 563–570. 10.1038/s41586-022-04585-5.

15. Wang, X., Tokheim, C., Gu, S.S., Wang, B., Tang, Q., Li, Y., Traugh, N., Zeng, Z., Zhang, Y., Li, Z., et al. (2021). In vivo CRISPR screens identify the E3 ligase Cop1 as a modulator of macrophage infiltration and cancer immunotherapy target. Cell *184*, 5357-5374.e22. 10.1016/j.cell.2021.09.006.